Chapter-II

Synthesis, Characterizations and Analysis Techniques

2.1 Overview

This chapter deals with the sample preparation techniques and experimental analysis to summarize the material's fabrication and characterizations along with the necessary theoretical background of the various structural and electrical parameters. This chapter also presents the techniques used for the sample preparation. In the present investigation, compositions were prepared via conventional solid state reaction route and chemical synthesis routes. Furthermore, prepared compositions were studied to characterise their structural, microstructural, thermal and electrical properties. This chapter is spanned out in three sections that revealed its significance in more proper fashion. The objective of first section is to discuss the detailed preparation and processing techniques that are involved in samples synthesis. The second section is highlighted for different characterization techniques like structural (XRD, FTIR, XPS), microstructural (SEM), thermal (DSC/TGA, TEC) and electrical properties (Impedance spectroscopy) which are utilized in the thesis work. Thereafter, third section introduces analysis techniques like X-ray Rietveld refinement, electrical conductivity and impedance spectroscopy, respectively.

In the following sections, the experimental techniques employed for the development and analysis of perovskite ($LaCrO_3$) and double perovskite ($Sr_2NiMoO_{6-\delta}$) electro-ceramic system in the presence of rare earth doped (Gd^{3+}, La^{3+}, Ce^{3+} and Sm^{3+}).

2.2 Synthesis and Characterization Processing of the Compositions

For the synthesis of a variety of compositions of high purity raw materials viz.: Chromium oxide, Lanthanum oxide, Gadolinium oxide, Ammonium molybdate, Nickel nitrate, Cerium nitrate, Samarium oxide and Citric acid have been used. The specifications of these materials are listed in Table 2.1. All investigated systems are also mentioned in Table 2.2.

2.3 Synthesis of Materials

2.3.1 Preparation of Nitrates

A few oxide materials (Gd_2O_3, La_2O_3, Ce_2O_3 and Sm_2O_3) are prepared via standard nitrate solutions techniques. Gd_2O_3 powder material was dissolved into dilute HNO_3 and solution was heated upto ~100 °C until appearance of $Gd(NO_3)_3$ crystal. The weighted La_2O_3 was dissolved into dilute nitric acid to get $La(NO_3)_3$ homogenous solution. In addition,

$Sm(NO_3)_3$ solution from Sm_2O_3 was also prepared by the same procedure as mentioned for $Gd(NO_3)_2$ and $La(NO_3)_3$, respectively.

Table 2.1: *Specifications of the raw materials with their grades, purity and manufacturer used for preparation of various electro-ceramic samples.*

S.N.	Raw Materials	Chemical Formula	Purity (%)	Manufacturer
1.	Lanthanum oxide	La_2O_3	99.9	Alfa Aesar
2.	Chromium oxide	Cr_2O_3	99.98	Alfa Aesar
3.	Gadolinium oxide	Gd_2O_3	99.9	Alfa Aesar
4.	Strontium nitrate	$Sr(NO_3)_2$	99.9	Alfa Aesar
5.	Nickel nitrate	$Ni(NO_3)2{\cdot}6H_2O$	99.8	Alfa Aesar
6.	Ammonium molybdate	$(NH4)_6Mo_7O_{24.}4H_2O$	99.9	Alfa Aesar
7.	Cerium nitrate	$CeN_3O_9.6H_2O$	99.5	Alfa Aesar
8.	Samarium oxide	Sm_2O_3	99.9	Alfa Aesar

Table 2.2: *Starting materials and firing schedule for various compositions.*

S.N.	Composition	Starting Materials (A.R. Grade)	Calcinations		Sintering	
			Temp. (°C)	Time (Hrs.)	Temp. (°C)	Time (Hrs.)
1	$LaCrO_3$	La_2O_3, Cr_2O_3	1000	5	1300	6
2	$La_{1-x}Gd_xCrO_3$	La_2O_3, Cr_2O_3, Gd_2O_3	1000	5	1300	6
3	Sr_2NiMoO_6	$Sr(NO_3)_2$, $Ni(NO_3)_2{\cdot}6H_2O$, $(NH4)_6Mo_7O_24.4H_2O$	1000	12	1300	24
4	$Sr_2Ni_{1-x}Mo_{1+x}O_6$	$Sr(NO_3)_2$, $Ni(NO_3)_2{\cdot}6H_2O$, $(NH4)_6Mo_7O_24.4H_2O$	1000	12	1250	24
5	$Sr_{2-x}La_xNiMoO_6$	$Sr(NO_3)_2$, $Ni(NO_3)_2{\cdot}6H_2O$, $(NH4)_6Mo_7O_24.4H_2O$, La_2O_3,	850	12	1350	12
6	$Sr_{2-x}Ce_xNiMoO_6$	$Sr(NO_3)_2$, $Ni(NO_3)_2{\cdot}6H_2O$, $(NH4)_6Mo_7O_24.4H_2O$, Ce_2O_3	900	12	1300	12
7	$Sr_{2-x}Sm_xNiMoO_6$	$Sr(NO_3)_2$, $Ni(NO_3)_2{\cdot}6H_2O$, $(NH4)_6Mo_7O_24.4H_2O$, Sm_2O_3	900	12	1300	12

2.3.2 Synthesis Routes

In order to process of materials, two different synthesis routes were adopted. The schematic presentations of the two routes are shown in Fig. 2.1.

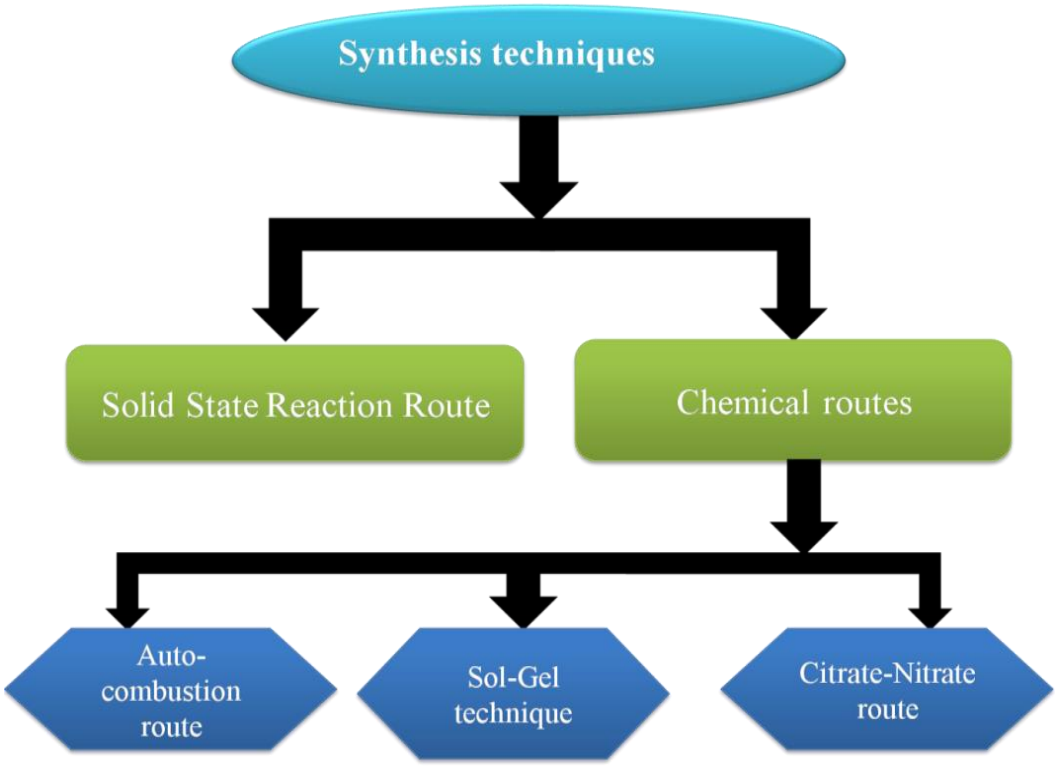

Fig.2.1: *Block diagram of various synthesis techniques.*

2.3.2.1 Solid State Reaction Route

Solid-state reaction method is the most extensively used method to synthesize the polycrystalline solids from a mixture of constituent oxides as starting materials. Care should be taken that solid oxides should not react at room temperature. Primarily, high purity raw materials (constituent oxides) in powder form are first weighed according to their stoichiometric ratio of the composition. The constituent oxides then mixed with appropriate weighed amount and grounded with mortar pestle for homogenous mixing. The mixed reactants are mixed in organic liquids like acetone/alcohol for homogeneity of compositions. For further mixing, a ball mill is employed for mechanical mixing process with desirable operating and time rate. The required phase formation is investigated after calcinations temperatures and kept at long holding time for sintering. The all steps of solid state reaction method are shown in Fig.2.2.

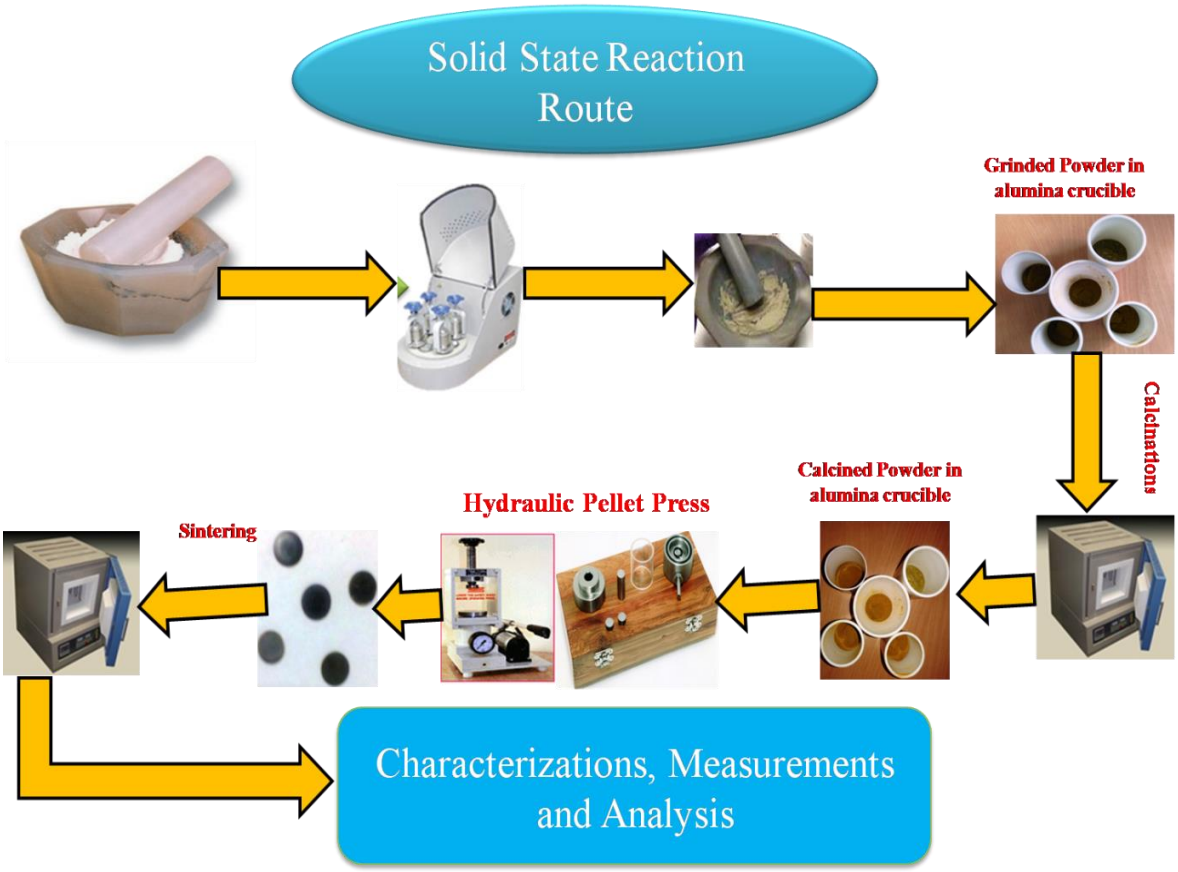

Fig.2.2: *The image diagram representing the steps of solid state reaction method.*

2.3.3.2 Chemical reaction routes

The chemical reaction route is fully-automated reaction techniques for all important reactions followed by the complex chemical reactions. This is mainly for controlling and reducing the particle size and other relevant purposes to change chemical and physical properties of used materials. Here we have used more than one independent complex chemical reaction methods: auto-combustion route, sol-gel technique and citrate-nitrate auto-combustion routes, respectively. Mostly nitrate materials were used for all chemical routes. In another process, a few oxides were used as nitrates after converting into nitrates with dissolving them into dilute nitric acid. In this method, we have presented an overview of the chemical reaction routes strategies and a few results of applications to examine their practical handling for systematic studies. The key stages in this route of sample preparation are calcinations and sintering. The sintering condition was optimized at high temperatures to achieve the desired phase. The working steps of chemical reaction route are shown in Fig.2.3.

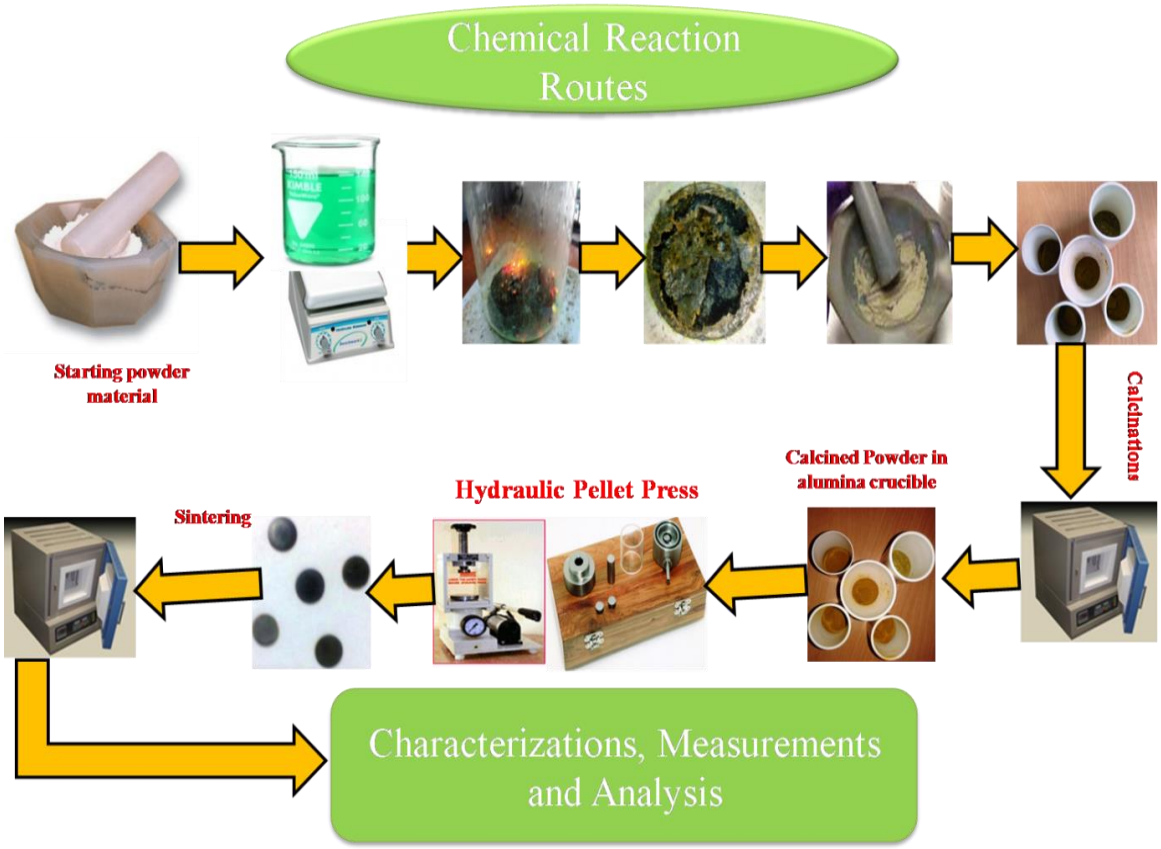

Fig.2.3:.*Diagram representation of chemical reaction route with the appropriate steps.*

(a) Auto-combustion route

Auto-combustion synthesis route has already been proposed in the study of many solid-state materials. It is previously studied that the properties and double perovskite systems are strongly influenced via the materials' composition and microstructure, which are very sensitive to the synthesis techniques [Prasatkhetragarn et al. (2012) and Singh et al. (2011)]. In various synthesis techniques such as sol–gel auto-combustion is relatively simple and fast process technique [Vijayakumar et al. (2009)]. In this process, high temperatures are attained in a short duration of a self-generated heat of reaction, yielding nanomaterials or loose agglomerates of nanocrystallites [Ringuede´ et al. (2001)].

(b) Sol-Gel technique

The sol-gel technique has been applied to a variety of perovskite and double perovskite systems ranging from room temperature to ~200 °C. This method is relatively simple, fast and effective method to convert monomers into a colloidal solution that proceed

to precursor solution [Ji et al. (2007)]. After drying precursor solution, a heating treatment was continued to get better mechanical process, while structural stability such as densification and crystal grain growth as well as electrical property is achieved through a final sintering process. Unlike to traditional processing methods, densification is frequently completed at much lower temperature from this method.

(c) Citrate-Nitrate Auto-combustion synthesis

Citrate-nitrate combustion synthesis is an easing processible going and convenient technique for the preparation of several advanced electro-ceramics materials [Xie et al. (2014)]. However, citrate-nitrate auto-combustion synthesis process had previously been used for perovskite and double perovskite systems, respectively. This synthesis technique is mainly utilized for two fold reasons, citric acid as a fuel where as metal nitrates are employed as metal and oxidant source. All desired nitrate precursors and citric acid were fully dissolved in distilled water to get a transparent homogenous solution. Furthermore, all prepared solutions were mixed together for homogeneity. To maintain the desired value of pH between 1 and 11, ammonia solution (40 wt. %) were added dropwise to the resultant solution. Finally, the resulting mixture solution was slowly evaporated on a hot plate having temperature 200 °C using magnetic stirrer. After passes of time, a solutions become gelled, foamed swelled & finally combusted. During evaporation, solution was changed into a gel of nitrate mixture and that nitrate mixture was slowly formed as swelled & auto-ignite violently. After self-ignition, a dried ash formed powder was obtained. The obtained powders were grounded into mortar and pestle for further necessary characterization techniques.

2.4 Characterizations techniques

This section describes the instruments/techniques employed for structural and electrical characterizations of all the prepared samples. A brief theoretical description of various characterizations techniques as XRD (X-ray powder diffraction), TGA/DSC (Thermo gravimetric Analysis/Differential scanning calorimetry), FTIR (Fourier transform infrared spectroscopy), SEM (scanning electron microscopy), XPS (X-ray photoelectron spectroscopy), thermal expansion coefficient (TEC) and impedance spectroscopy, is presented here. The block diagram of all above characterization and analyses techniques is shown in Fig.2.4.

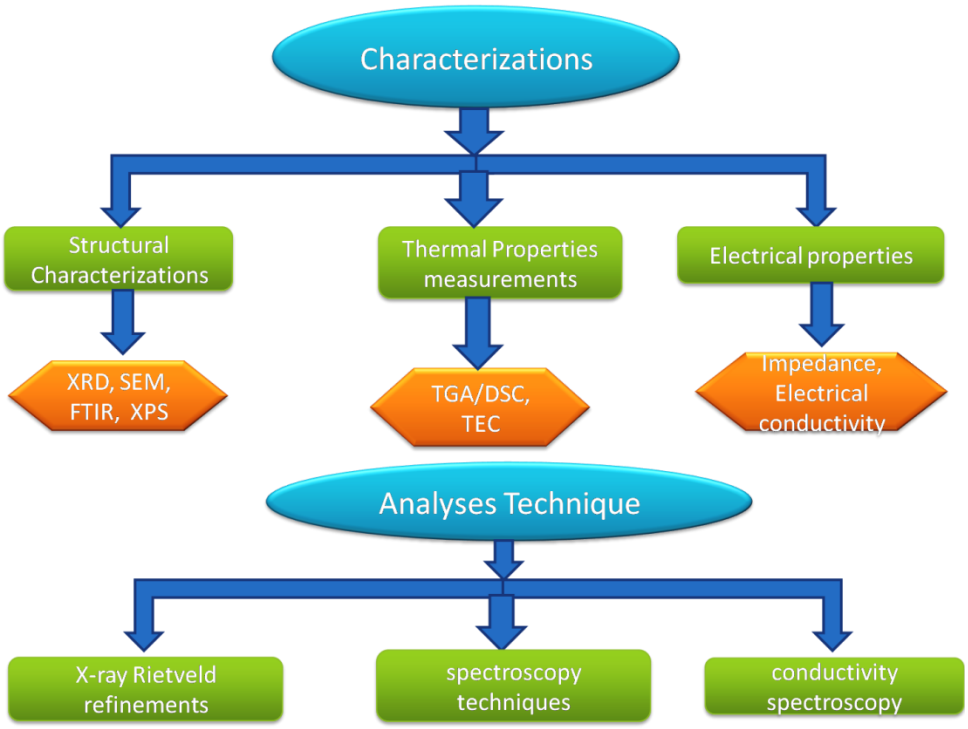

Fig.2.4: *Block diagram of various characterization and analyses techniques.*

2.4.1 Phase Formation and Crystal Structure Studies by Powder X-Ray Diffraction

A primary utilization of the X-Ray technique is for the phase identification and characterization of prepared materials in their diffraction pattern. X-ray diffraction (XRD) shows dual wave/particle nature of X-rays to attain information about the crystal structure of materials. X-ray crystallography is a tool that measures the angles and intensities of diffracted beams to observe the three-dimensional image of the density of electrons contained by the crystal. X-ray radiations are generally emitted by copper element along with its characteristic wavelength for the Cu-K_α radiation is ≈1.5418 Å. When the beam is incident on a target a powder sample, sample and detector are rotated in 2θ orientation and diffraction peaks are recorded in term of intensity. The X-ray diffraction profile is used to determine the atomic arrangements in the materials because the inter-planar spacing (d) of the diffracting planes is of the order of X-ray wavelength λ. For a crystal of given inter-planar spacing (d) and wavelength λ, the various orders n of reflection occurs only at a precise angle θ, which satisfies the Bragg condition: $2d \sin\theta = n\lambda$ is shown in Fig.2.5.

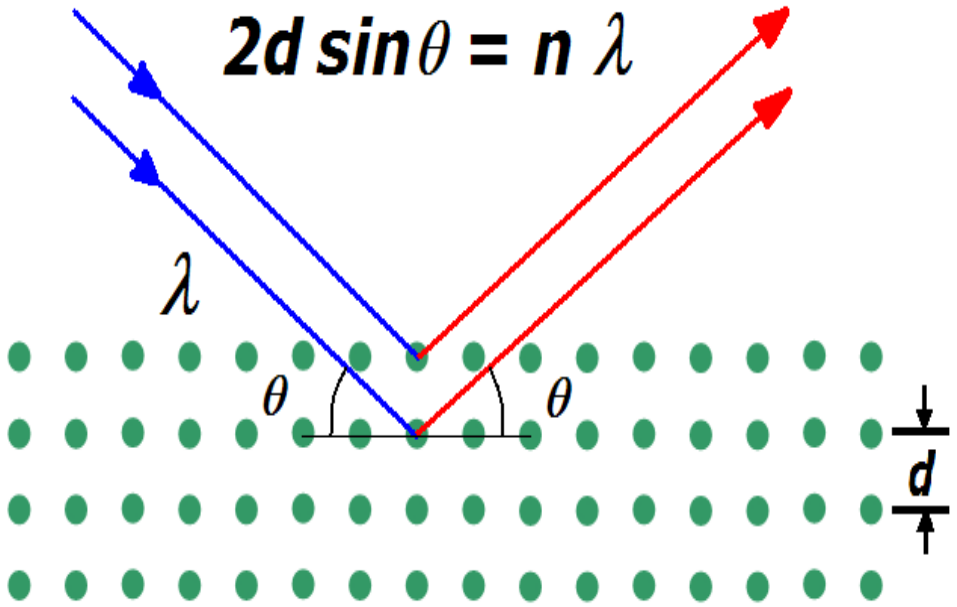

scienceaddomesticity.wordpress.com

Fig. 2.5: *Schematic diagram of Bragg's law occurring through a crystal lattice.*

The mean positions of atoms in the crystal as well as their chemical bonds (bond angle, bond length), crystallite size, strain and various other information can be determined from the XRD pattern. In the X-ray system operation, the counter is arranged to scan over a range of 2θ values along with constant angular velocity. The basic principle of X-ray diffraction is to investigate the structural, physical and chemical information of the target material. The single or multiple phase identification of an unknown material is one of the important applications of X-ray powder diffractometry. Moreover, the phase detection also supports or discloses to understand the mechanism of formation of these materials and reveals its specific details. A powder diffraction technique has played an important role into structural physics, materials science and chemistry in determining the crystal structure of a solid into both organic and inorganic types. The X-ray measurement setup with working diagram is shown in Fig.2.6. In the present study, to confirm the single phase formation, powder XRD was done at different stages (i.e. as self ignited ash, calcined and sintered) of synthesis and processing of prepared samples. The obtained voluminous powder was ground using mortar and pestle after that calcined and sintered pellets were reground to record powder XRD

pattern by using an X-ray Diffractometer (Rigaku Miniflex II, desktop) employing Cu-$K\alpha_1$ radiation with Ni filter. The single-phase formation of the as prepared ceramic samples was authenticated by the absence of characteristic lines of constituent oxides or any other phase observed in the XRD patterns. The XRD patterns were indexed via JCPDS cards of PCPDFWIN program and lattice parameters were also determined using least square fitting of the recorded data using a software 'unit cell' program.

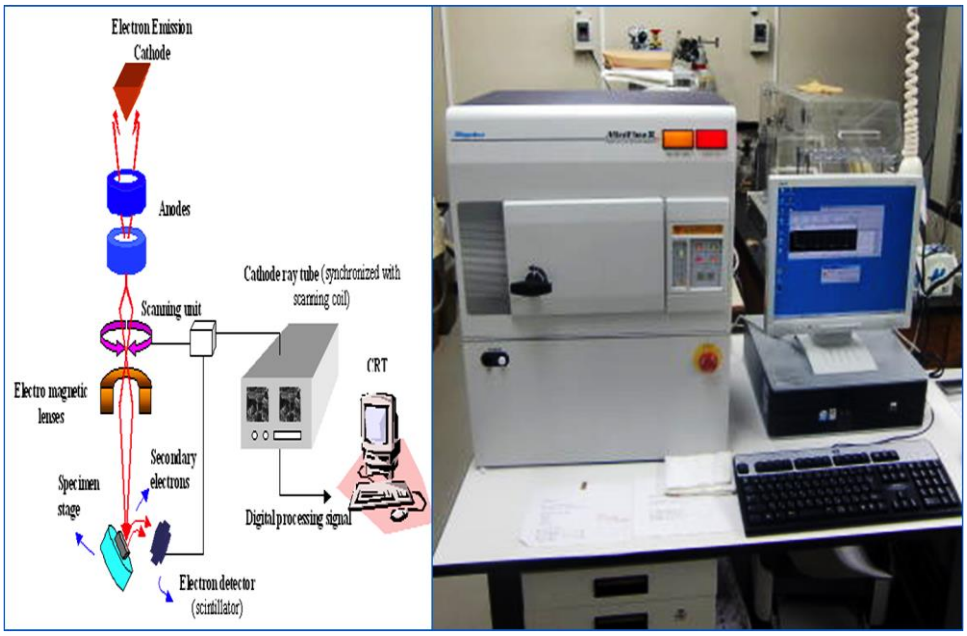

Fig. 2.6: *X-ray diffractometer working representation with image of Rigaku (Miniflex II desktop).*

The average crystallite size was estimated by X-ray line broadening analysis using Scherrer's formula.

$$D = \frac{0.9\lambda}{\beta_c \cos\theta} \qquad (2.1)$$

where λ is the wavelength of X-ray diffraction peak, β_c is corrected full width at half maxima of the diffraction peak and θ is Bragg's diffraction angle.

2.4.2 Density and Porosity Measurements

There are various manual and automated techniques to determine the experimental density of the sintered pellets. In this chapter, the experimental density was measured by Archimedes principle using water as a liquid medium. This method is the useful context of

economically viable as well as time saving. The density measurement setup is shown in Fig.2.7.

Fig 2.7: *Photograph of density kit of Mettler-Toledo.*

Theoretical density was calculated from the molecular weight of the given compound and lattice parameters as

$$D_{th} = \frac{n \times M}{N \times V} \quad (2.2)$$

where D_{th}, n, M, N and V are theoretical density, a number of formula unit per unit cell, a molecular weight of given sample, Avogadro's Number and unit cell volume, respectively. The standard method for percentage porosity was directly calculated using the relation

$$\text{Percentage } porosity = \left(\frac{D_{th} - D_{exp}}{D_{th}}\right) \times 100 \quad (2.3)$$

where D_{th} and D_{exp} are the theoretical density and experimental density, respectively.

2.4.3 Microstructural Studies by Field Emission Scanning Electron Microscopy (FESEM) and Electron Dispersive Spectroscopy (EDS)

Scanning Electron Microscope (SEM) is the most important technique to examine the microstructure of ceramic samples using focused electron beam on target materials. A cathode electron gun of a scanning electron microscope provides finer probing beams at low and high electron energy to improve the resolution and minimize the sample charging and damage. In vacuum atmosphere, electrons generated by a field emission source, are accelerated under a

field gradient. The applied electron beam scanned microstructure images are detected which contains the information about the sample's surface. To obtain clear visible and better contrast of SEM micrographs, samples must be electrically conductive at the surface and electrically grounded to prevent the accumulation of electrostatic charge at the surface. In the most common SEM mode, a detector catches the secondary electrons that are emitted by atoms excited by the electron beam. Finally, the micrograph images are displayed on the monitor. FESEM makes clearer images and less electrostatically distorted images with resolution up to 1-2 nm. EDS is generally attached with SEM, which provides elemental information with peak reflection in energy distribution curve of characterise materials. The atomic number of the content element should be greater than boron and concentrations of detectable element at least order of 0.1 percent to identify the elemental composition of materials. The high-resolution FESEM permits the study of surface morphology analysis (Particles shape and size) and microstructural information such as grain orientation, texture and phase detection, fractured analysis and interface behaviour as well as qualitative element analysis.

In order of FESEM characterization, sintered pellets were polished using emery papers of various grades as 1/0, 2/0, 3/0, 4/0 and 5/0 (Sia, Switzerland) sequentially after that these were chemically etched. The surface morphology was recorded using, ZEISS scanning electron microscope (EVO-18). A field emission scanning electron microscope ZEISS (EVO-18) was used to test out the surface micrograph of the compositions is shown in Fig.2.8.

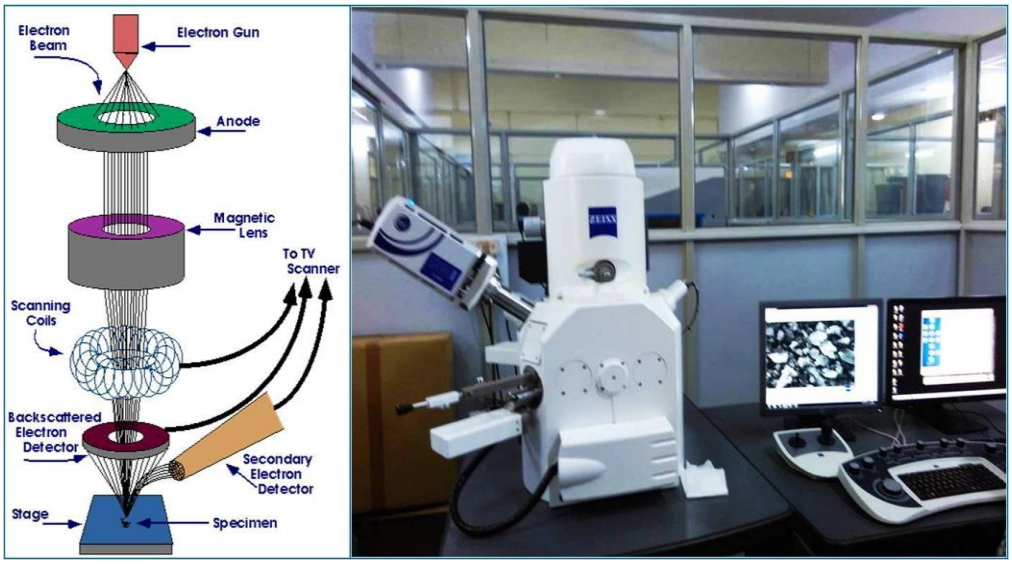

Fig.2.8: *Schematic diagram representation of SEM (scanning electron microscope) with image of ZEISS (EVO-18).*

2.4.4 FTIR Measurements

FTIR (Fourier transform infrared spectroscopy) is an important technique for materials analysis to exploit an infrared spectrum of absorption or emission of a liquid, solid or gas. FTIR technique makes the most of the fact that the occurrence of molecules absorbs specific frequencies along with their structure characteristic. A few infrared radiations may be absorbed by the prepared sample and some of its radiation could be transmitted. A Shimadzu spectrometer setup with KBr dilution was used to record the absorption bands in the range of 4000– 400 cm^{-1}. Besides absorption bands, stretching modes of vibrations have also been studied with respective peak intensity. The working photograph of FTIR measurements setup of Shimadzu spectrometer (FTIR-8400S) is shown in Fig.2.9.

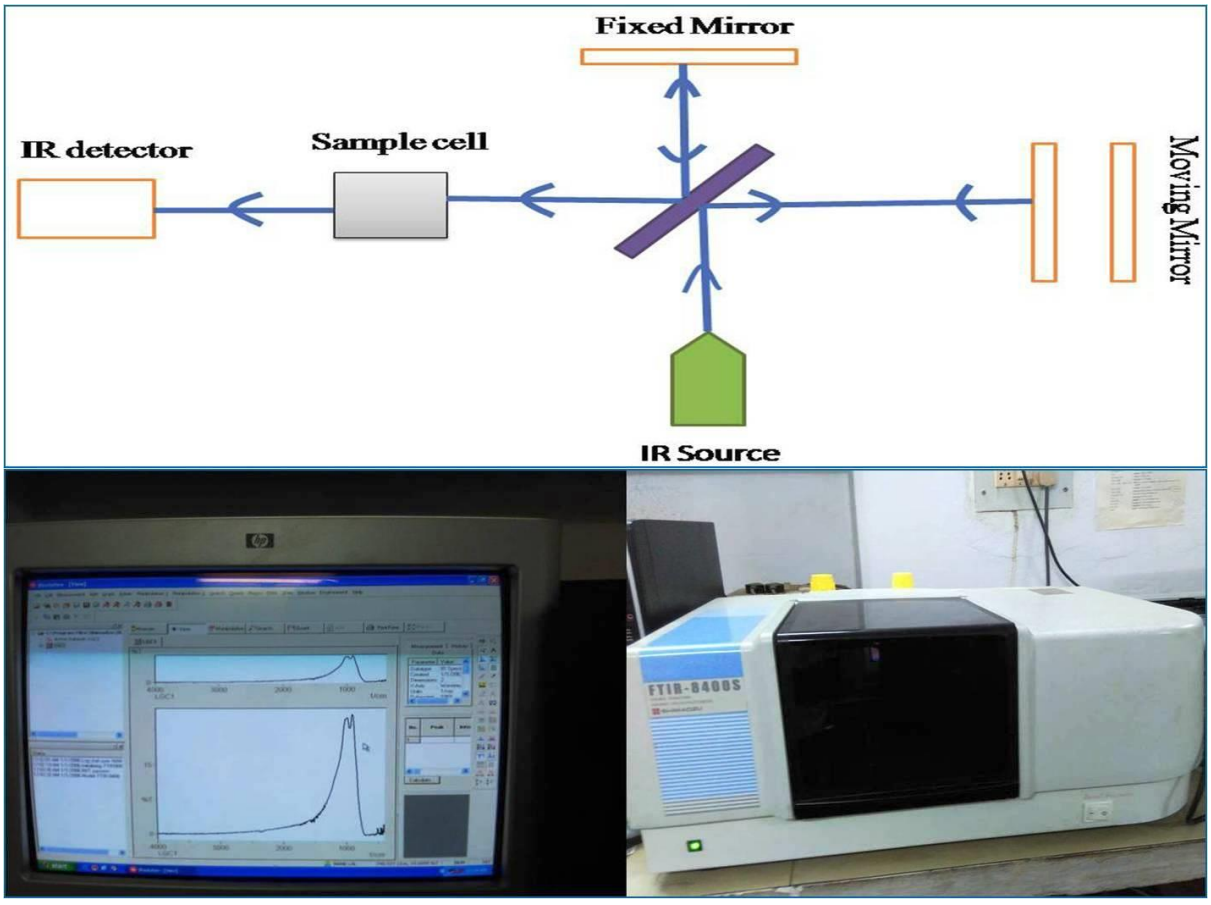

Fig 2.9: *Schematic diagram of FTIR spectrometer working with photograph of Shimadzu spectrometer (FTIR-8400S).*

2.4.5 X-ray Photoelectron Spectroscopy

XPS (X-ray photoelectron spectroscopy) is the most widely used surface analysis technique to study the surface chemistry of a material of each element, their chemical states and electronic states that exist within a material. XPS analysis is not only providing the presence of elements, but also detects the binding energy of emitted electrons which can provide chemical bonding information. Excited electrons are emitted from the parent atom as photoelectrons if their binding energy is lower than the X-ray energy. Each element possesses a characteristic peak of binding energy that is indicated in a binding spectrum by analyzer with the corresponding electron configuration of the atoms like 1*s*, 2*s*, 2*p*, 3*s*, etc. The number of detected electrons in each of the characteristic peaks is directly related to the amount of element within the XPS sampling volume.

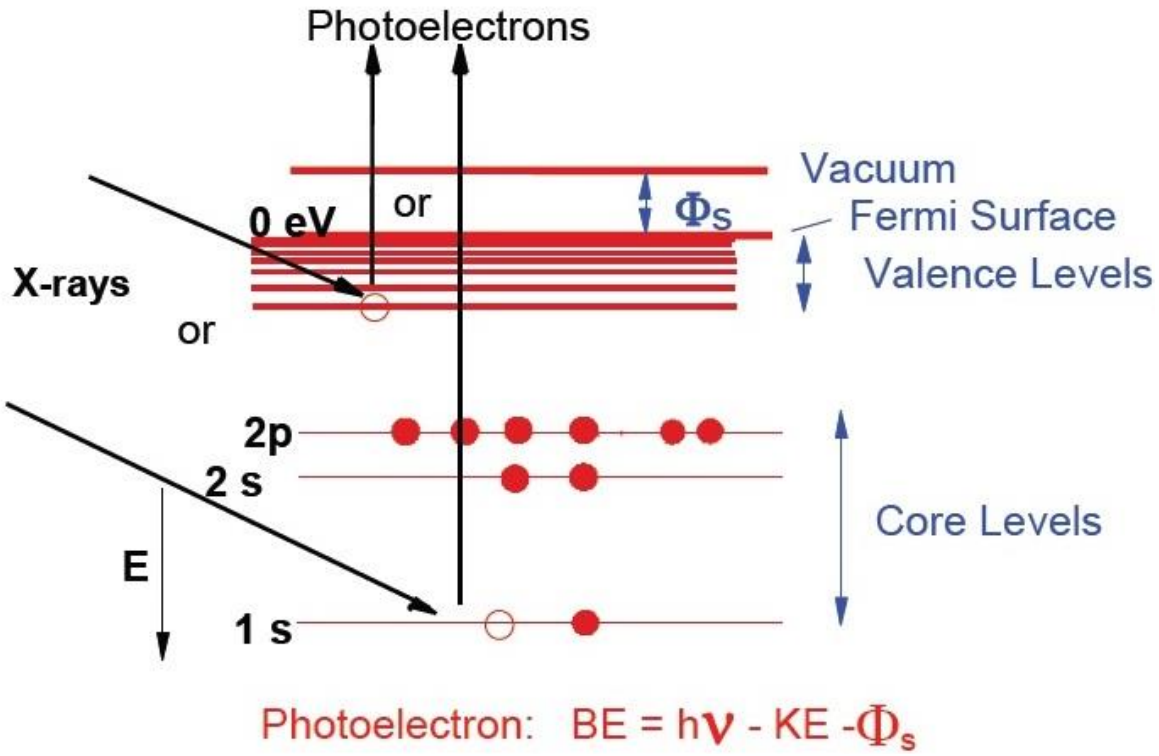

Fig.2.10: *Schematic diagram of XPS (X-ray photoelectron spectroscopy).*

In basic principle, the energies of the photoelectric lines are well described in terms of the binding energy of the electronic states of atoms (see Fig. 2.10). The chemical states of the atoms at the surface result are in well-identified energy shifts to the peak energies. In the

study of conducting samples, the detected electron energies can be referenced to the fermi energy of the spectrometer; an absolute energy scale can be established for identification of species.

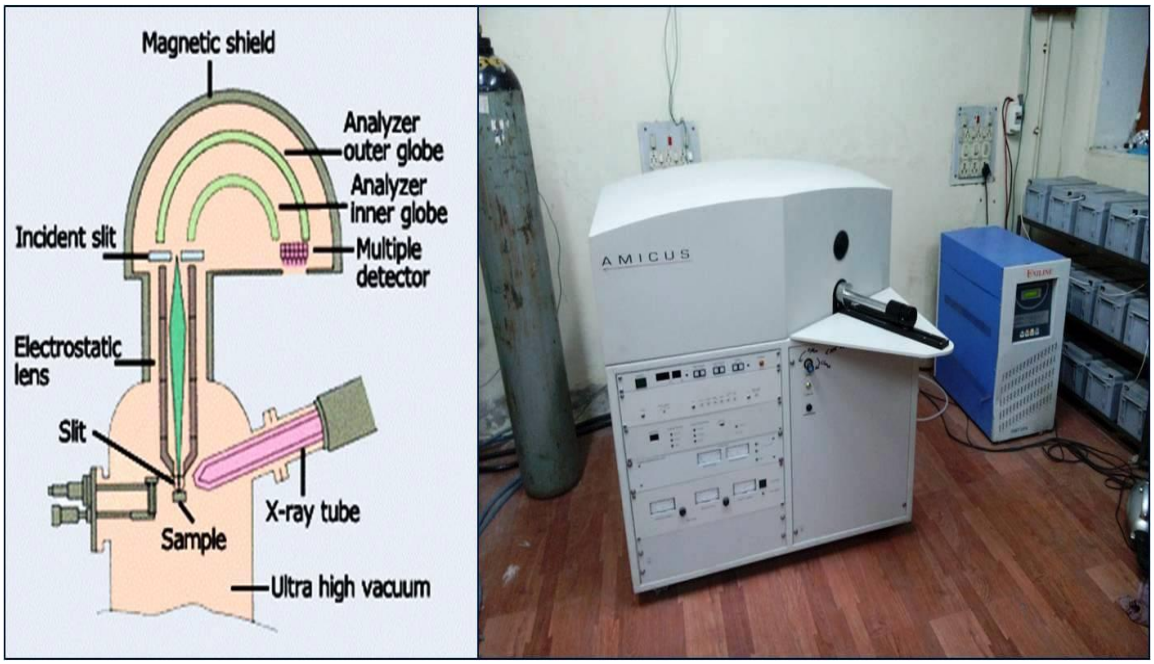

Fig 2.11: *A Schematic design of XPS (X-ray photoelectron spectroscopy) working with photograph of XPS setup (KRATOS Amicus model).*

An Amicus XPS setup was utilized to perform elemental analysis and chemical states of the given compositions as presented in Fig.2.11.

2.4.6 Differential Scanning Calorimetric (DSC) and Thermo Gravimetric Analysis (TGA)

DSC/TGA (Differential Scanning Calorimetric/Thermo Gravimetric Analysis) both are thermo analytical techniques with weight change and heat flow measurement under identical conditions. The block diagram of DSC/TGA with measurement setup is shown in Fig. 2.12. The basic principle of DSC technique is based on the fact that the sample goes through a physical transformation similar to phase transition conditions more or less heat will be required to flow in such a way to keep the reference temperature to retain both at the same. Exothermic or endothermic reactions also play a key role in the appropriate amount of heat flow for crystallisation and phase transition process.

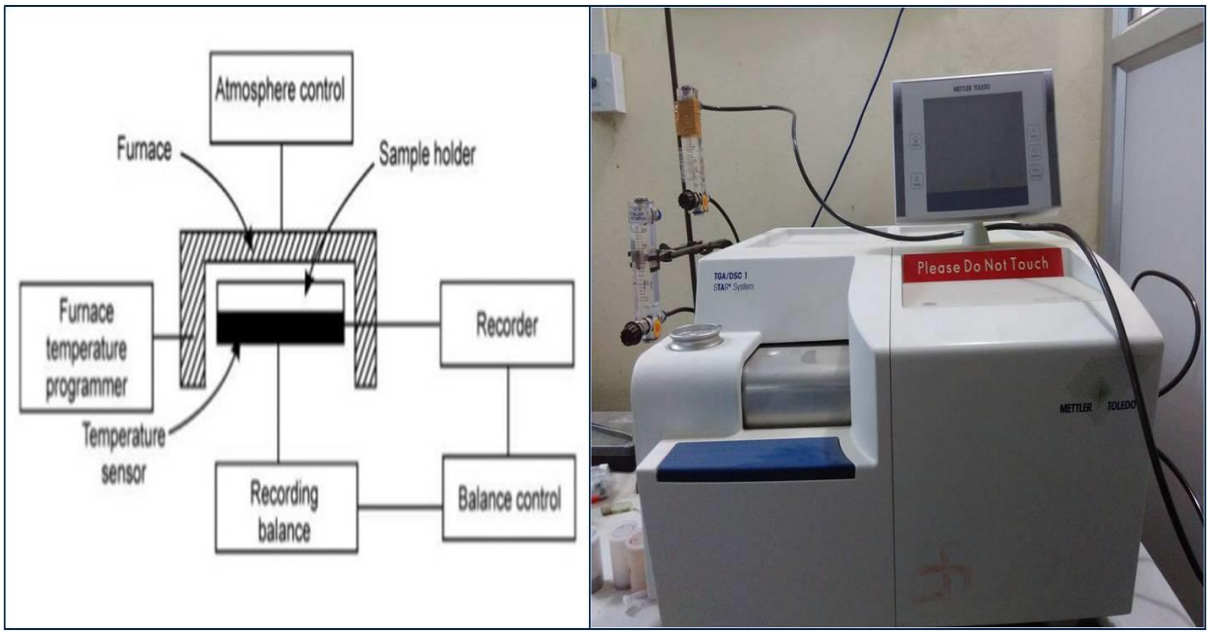

Fig 2.12: *Block diagram of DSC/TGA measurement along with setup image of Mettler Toledo (TGA/DSC1 STAR^e thermal analyzer).*

DSC technique can be used to measure numeral characteristic properties of a sample like fusion, crystallization and glass transition temperatures T_g**.** DSC is widely used to study polymeric materials, liquid crystals, Oxidative stability and in pharmaceutical industries. In present study, DSC analysis shows heat flow between the sample and reference with respect to temperature variation of as prepared and sintered compositions.

TGA is an important technique in various thermal analysis techniques in which a change of physical and chemical properties of materials are evaluated as a function of temperature at constant heating rate and function of time at a constant temperature or mass loss. It provides the basic characteristics of selected materials like mass gain or loss due to decomposition, oxidation, reduction or loss of volatiles similar as moisture. The prepared sample of a few milligrams is weighted heated at a constant rate (in the range of 1 to 20 ^oC min^{-1}) and has an invariable weight until it goes to decompose at a certain operating temperature.

2.4.7 Thermal Expansion behaviour

The thermal expansion coefficient (TEC) is a basic physical property that is used in mechanical and structural design applications of ceramic materials. The physical thermal

expansion coefficient (α) can be calculated from the slope of relative length–variation curve at a given temperature (T) by the following equation

$$\frac{dL_0}{L_0} = \alpha(T) \times \Delta T \qquad (2.4)$$

where L_o represents the initial length of the sample. Thermal expansion is the physical process of matter that changes in shape, dimensions (length), area, and volume with change in temperature via heat transfer. In principle, the reference material measures the fractional change in size over the temperature range of interest. In the application of SOFCs (Solid Oxide Fuel Cells), TEC is one of the important parameters for the materials used as cell components to prolong the life of cells and components of the cell should be thermally compatible. The TEC measurement setup with working representation is shown in Fig.2.13.

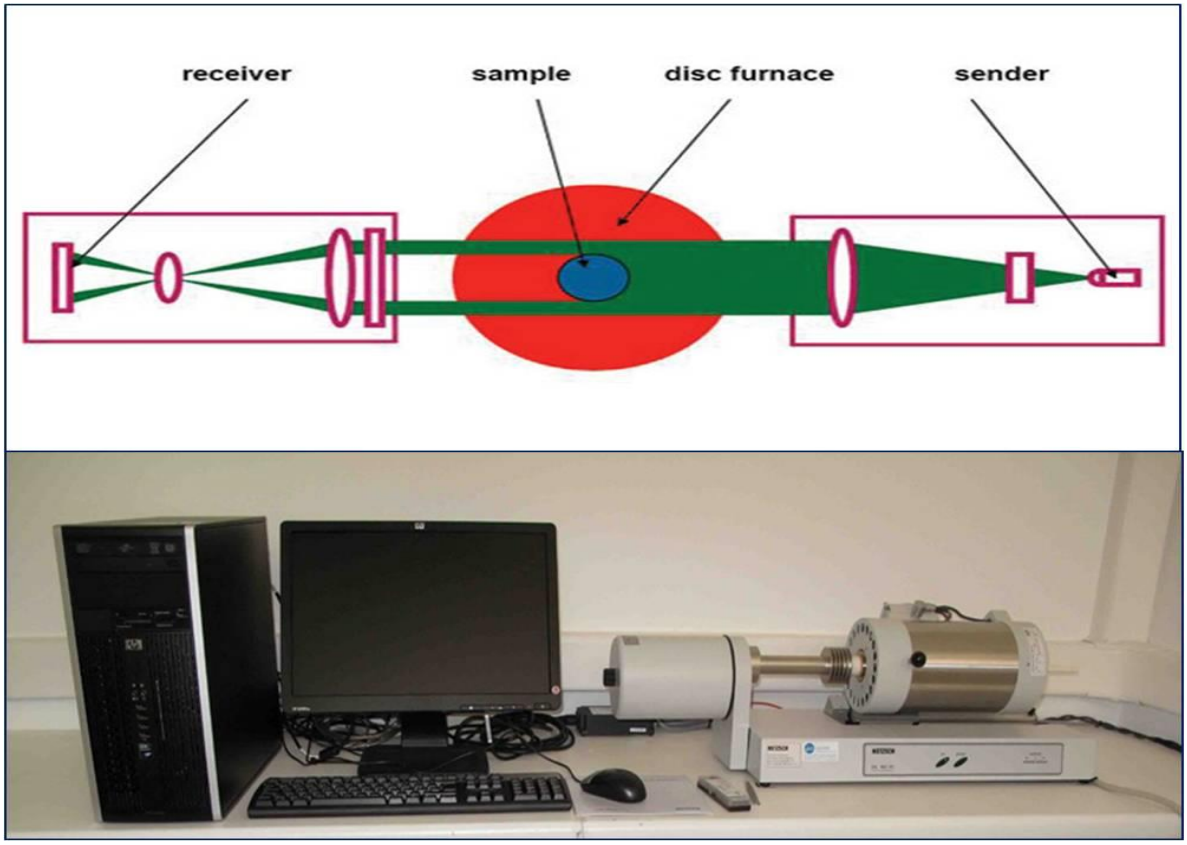

Fig.2.13: *A design of working and its corresponding photograph of dialatometry setup for TEC measurement (DIL 402 PC, NETZSCH).*

2.5 Conductivity Measurement

2.5.1 Conductivity Measurement in Air Using Impedance Analyser

Various methods have been suggested to measure the electrical conductivity. Among them two probes (ohmmeter or voltmeter–ammeter measurements) can be used for higher resistive samples and four probes methods (potential probe measurements) for the low resistive samples. Two probes measurement is the relatively simplest method of measuring conductivity. This method is practically useful when the sample has a large resistance. In this method, conductance is measured across the voltage drop V across the sample and current through the measured sample. The electrical measurement is investigated by sintered pellets-which are polished with the help of emery papers of grade order 1/0, 2/0, 3/0, 4/0, 5/0 (Sia, Switzerland) and after that silver (Ag) paste was coated on both surfaces of the pellets. These coated pellets were cured at 750 °C for 30 minutes. The impedance measurements of the real and imaginary parts i.e. Z' and Z'' of different samples were carried out on silver coated electrodes pellets using two probe method in the frequency range 20 Hz to 5 MHz and at an interval of 25 °C from room temperature to 700 °C in air using a Wayne Kerr 6500 P impedance analyzer. AC impedance measurements were evaluated through PID controlled electric furnace along with sample holder. The measurement setup of Wayne Kerr 6500 P impedance analyzer is shown in Fig.2.14.

Fig. 2.14: *Computer controlled automated impedance analyser setup along with sample holder and furnace (6500 P Wayne Kerr, UK).*

2.5.2 Electrical measurements in reducing atmosphere using Probostat

The electrical measurements in reducing atmosphere were carried out using the Probostat (Norecs, Norway) system. The Probostat system (Figure 2.15) permits to study the electrical properties of materials used for the manufacture of fuel cells, complete cells testing or its parts (cathode, electrolyte and anode). This instrument consists of assembled parts made of ceramic material (like alumina), which is suitable to resist high temperatures and that, given its inert nature, allows the use of various gases without the danger of unwanted reactions. This instrument is divided into two basic parts: the lower part and outer part. The lower part hexagon, which is made of steel and nickel-plated brass, has the function to accommodate the electrical and power connections and exhaust of gas input and output from the device; the reaction section, made of alumina is characterized by an inner and an outer compartment and allows the housing and fastening of the sample.

Fig.2.15: *The Probostat (Norecs, Norway) system impedance Analyzer (FRA, mod. SOLARTRON 1250 - Schlumberger), in a range of frequency between 10^{-1} – 10^{5} Hz.*

The outer part is consisted with four Pt electrodes, connected by Pt wires to impedance meter to read the potential and the current during the; one thermocouple for a correct estimate of the sample temperature during the tests; a system of springs for mechanical load of samples: a tube used to seal the outer compartment. The impedance measurements could be done with electrochemical interface (EI, mod. 1286 - Schlumberger) used in potentiostatic mode and connected to a Frequency Response Analyzer (FRA, mod. SOLARTRON 1250 - Schlumberger, Fig. 2.15), in a range of frequency between 10^{-1} – 10^{5} Hz.

2.6 Analysis Techniques

2.6.1 Phase formation study by Rietveld Refinement technique

The Rietveld technique is a more widely used technique to determine the phase purity, crystal structure and lattice parameters. The Rietveld method along with a modelling of the peak profile is extremely useful for the study of metastable and mixed phase form of given materials. Due to an existence of crystal structural defects like dislocations, stacking faults, anti-phase domains, micro-strains and small crystallite sizes apparent in the diffraction pattern by a broadening of the Bragg peaks [Carvajal (2002)]. Generally, the Voigt approximation for peak broadening is sufficient to acquire quantitative explanation of the presenting defects through the different lattice planes (hkl) and angular dependence of the peak broadening.

The Voigt approximation is based on the assumption that the convolution of the various effects has been found to result in a Gaussian shape. If this distribution is taken then the contribution of a given reflection to the profile y_i at position $2\theta_i$ is

$$y_i = I_k \exp\left[\frac{-4\ln(2)}{H_k^2}(2\theta_i - 2\theta_k)^2\right] \quad (2.5)$$

where H_k is the full-width half-maximum, $2\theta_k$ is the centre of the reflex, and I_k is the calculated intensity of the reflex that can be determined from the structure factor, Lorentz factor and multiplicity of the reflection. At very low diffraction angles the reflections could be attained an asymmetry which occurs due to the vertical divergence of the beam. Rietveld refinement also draws a semi-empirical correction factor,

$$A_s = 1 - \left[\frac{sP(2\theta_i - 2\theta_k)^2}{tan\theta_k}\right] \quad (2.6)$$

The width of the observed diffraction peaks is originated to broaden at higher Bragg angles. This angular dependency was originally represented in terms of FWHM parameters

$$H_k^2 = U\ tan^2\theta_k + Vtan\theta_k + W \quad (2.7)$$

where *U*, *V* and *W* are the FWHM parameters, they are refined during the peak fitting. The basic principle of the Rietveld refinement is to minimize a function *M* that can be analysed the difference between a calculated profile y_{cal} and the observed data y_{obs}

$$M = \sum_i\ W_i \{y_i^{obs} - \frac{1}{c} y_i^{cal}\}^2 \quad (2.8)$$

where W_i is the statistical weight and c is an overall scale factor such that $y^{cal} = cy^{obs}$ program is suitable software to study the Rietveld refinement. The program has been basically developed for Rietveld analysis [Rietveld, et al. (1967 and 1969); Hewat, (1973), Malmros et al. (1977) and Khattak et al. (1977)] (peak profile refinement) of neutron diffraction pattern (nuclear and magnetic scattering) or X-ray powder diffraction data refined at constant or variable step in scattering angle 2θ. In the current study, we give most of the information to the treatment of microstructural effect employing the FullProf program. The peak profiles were modelled by using pseudo-voigt function and back ground has been described in terms of twelve coefficient polynomials. The R_{wp} (weighted-pattern factor), R values (Rp), $\chi 2$ values and S (goodness-of-fit) parameters were used as a numerical criterion of quality of the fit of calculated to experimental diffraction data. The structural parameters of the powders were investigated by the Rietveld analysis of XRD data applying the FullProf software.

2.6.2 Conductivity Spectroscopic Technique

Electrical conductivity spectroscopy is a most useful technique to investigate electrochemical properties of the mixed conductors (ionic and electronic). The electrical conductivity is measured in two regimes dc and ac conductivity σ_{dc} & $\sigma_{ac,}$ respectively. The σ_{dc} of polycrystalline materials assume only single dynamic response with frequency independent behaviours. Generally, conductivity measurements are operated with dc bias over the materials which show the polarisation at the electrode/electrolyte interface of the material. In polycrystalline materials, electrical conductivity relaxation arises with contributions grain, grainboundary, and electrode-specimen interface. In case of electro-ceramics, frequency dependant conductivity spectra distinguish into two dispersion regime, low frequency regime (or frequency independent regime) plateau that represents DC conductivity while at high

frequency, frequency dependent dispersive region represents AC conductivity. Both regions are attributed to combined effect of grain and grain-boundary relaxation in absence of electrode polarisation processes. The DC conductivity of the system was evaluated from the low frequency plateau of the conductivity spectra and is represented in Arrhenius fashion which shows relatively low value due to electrode polarisation dominating at low frequencies. The conduction mechanism is studied in two parts: the frequency-independent part allotted to the dc conductivity which caused by the random motion of the mobile charge carriers, and the frequency-dependent part (dispersion regime) assigned to the ac conductivity due the hopping motion of the mobile charge carriers in grains and grainboundaries. In most polycrystalline ceramic materials the frequency dependent real part of the conductivity spectra is given by

$$\sigma' = \sigma_{dc} + \sigma_{ac}, \quad (2.9)$$

where the ac conductivity ($\boldsymbol{\sigma}_{ac}$) can be write with general formula

$$\sigma_{ac}(v, T) = A(T).v^{p(T)} \quad (2.10)$$

where, A is a constant and also depends on various factors. The real part of electrical conductivity σ' can be described applying of Jonscher power law.

$$\sigma' = \sigma_{dc}\left[1 + \left(\frac{\nu}{\nu_H}\right)^p\right], \quad (2.11)$$

where, ν_H parameter is the hopping frequency, ν is the frequency and p is exponent factor that can be found to be less than unity.

2.6.3 Impedance Spectroscopic Technique

Impedance Spectroscopy (IS) is an effective and simple tool to study the electrical properties of the polycrystalline materials. It facilitates the tailoring of polycrystalline materials by separating out the contribution of different parts i.e. grain, grainboundary and electrode specimen interface to the electrical conductivity. The electrical and dielectric properties of polycrystalline electronic ceramics have three contributions (i) grains or bulk (ii) grain boundaries and (iii) electrode polarisation interface. Impedance spectra are composed of three depressed semi-circular arcs which are characteristic to grains or bulk, grain boundaries and electrode polarisation respectively. It is necessary to separate these contributions. Primarily, the observed difference in capacitances can be separated the contribution of observed semicircular arcs. The capacitance corresponding to observed semicircular arc was

calculated by the relation $2\pi fRC=1$, where *f*, R and C are peak frequency, resistance and capacitance, respectively, which holds good at the peak of the corresponding semicircular arc.

Impedance study has emerged as a simple tool to separate the various contributions consists of the electrical/ dielectric properties of electronic ceramics [Hench (1968); Hodge et al. (1976) and Macdonald (1987)]. It is a functional tool to study defects, microstructure, surface chemistry and electrical conductivity of polycrystalline ceramic materials to explore a different kind of properties such as dielectrics, ionic conductors and adsorbate-adsorbent interface. AC response of the materials can be expressed by any of the four basic formulas. These are complex impedance (Z^*), admittance (Y^*), electric modulus (M^*) and permittivity (ε^*) jointly referred to as spectroscopic functions which are expressed the following relation

Complex impedance: $$Z^* = Z' - iZ'' = \frac{1}{i\omega C_0 \varepsilon^*} \quad (2.12)$$

Complex Admittance: $$Y'' = Y' + iY'' = i\omega C_0 \varepsilon^* \quad (2.13)$$

Complex modulus: $$M^* = M' + iM'' = \frac{1}{\varepsilon^*} \quad (2.14)$$

Complex permittivity: $$\varepsilon^* = \varepsilon' - i\varepsilon'' \quad (2.15)$$

Each is correlated among various parameters can be described as follows:

$$D = \tan\delta = \frac{\varepsilon''}{\varepsilon'} = \frac{M''}{M'} = \frac{Y'}{Y''} = \frac{Z'}{Z''} = \frac{\sigma'}{\sigma''} \quad (2.16)$$

$$Z' = \frac{D^2}{G \cdot (1+D^2)} \quad , \quad Z'' = \frac{Z'}{D} \quad (2.17)$$

$$\sigma' = \omega\varepsilon_0\varepsilon'' \text{ and } \sigma'' = \omega\varepsilon_0\varepsilon' \quad (2.18)$$

where, ω is the angular frequency ($\omega=2\pi f$) of applied electric field, f being the frequency in cycles/sec, C_0 is known as the geometrical capacitance. Z*, Y* and M* are generally used in the analysis of electrical/dielectric properties of electronic ceramic materials. These parameters are plotted in form of complex plane plots e.g. Z″ vs. Z′, M″ vs. M′ and spectroscopic plots Z″ or M″ vs. log ν. If electro-ceramics have a contribution of grains, grainboundaries and electrode, then each of them can be represented by a circuit element diagram containing R and C connected in parallel. Therefore these are represented by an

equivalent circuit containing three parallel RC circuit elements functioning in series as shown in Fig 2.15.

Nyquist plots (Cole-Cole plots) are usually plotted to explain frequency response information of a system by complex impedance function $Z^*(\omega) = Z'(\omega)-iZ''(\omega)$, where $Z'(\omega)$ and $Z''(\omega)$ are the real and imaginary parts of $Z^*(\omega)$. The real part of impedance (Z') and imaginary part (Z") are defined as

$$Z' = \frac{R_g}{(1+\omega R_g C_g)^2} + \frac{R_{gb}}{(1+\omega R_{gb} C_{gb})^2} \quad (2.19)$$

$$Z'' = R_g \frac{\omega R_g C_{gb}}{(1+\omega R_g C_g)^2} + R_{gb} \frac{\omega R_{gb} C_{gb}}{(1+\omega R_{gb} C_{gb})^2} \quad (2.20)$$

where R_g and C_g are the bulk (grain) resistance and capacitance, respectively, and R_{gb} and C_{gb} are the corresponding quantities for interfacial boundary (grainboundary). The relative intercept position of the two semicircular arcs in a complex plane can be identified by frequency. The arc of bulk indicates higher frequency than that of interfacial boundary since the relaxation time for the interfacial boundary is much larger than that for the bulk crystal. Therefore, when the bulk resistance (R_g) is much lower and the resistance in the equivalent circuit is lead by the interfacial boundary resistance (R_{gb}), the arc of bulk (grain) may be in the limited frequency range. Resistance R_g, R_{gb} and R_{el} have symbolized the resistive contributions of grains, grainboundaries and electrode polarization process while C_g, C_{gb} and C_{el} symbolise their corresponding capacitive contributions, respectively. The analysis of complex plane impedance and modulus spectra are observed three semicircular arcs with their intercepting points on the real axis which have a single value of relaxation time as shown in Fig. 2.16.

Relaxation time τ inversely proportional to angular frequency, ω at which the relaxation peak occurs, is given by the RC product i.e.

$$\tau = 1/\omega = RC \quad (2.21)$$

Hirose and West et al. [1996] also reported the equations for the real axis intercepts for various immittance functions in complex plane plots.

The intercepts of the arcs on M′ axis in modulus plots are inversely proportional to the capacitance value (C_o/C_g, C_o/C_{gb} and C_o/C_{el}). The capacitance value from the impedance plots and resistance from the modulus plots can be observed from the peak frequency point in the arc by the relation $\omega RC = 1$. The entire measured frequency increases in opposite direction in

complex plane impedance of modulus plots. The electrode polarization process is very slow-moving that appear in the lowest frequency range followed by grainboundaries in the intermediate frequency range and bulk or grains contribution appears in the highest frequency range in the impedance spectra. The considerable number of arcs appearing in the complex plane plots which also depends on the ratio of various time constants. An electro-ceramics also having the negligible value of electrode-interface contribution can be represented by two parallel RC elements connected in the series circuit. Grain and grainboundary conductivities σ_g and σ_{gb}, could be determined using relations $\sigma_g = (1/R_g)\cdot(t/A)$ and $\sigma_{gb} = (R_gC_b / R_{gb}C_{gb}).\sigma_g$ respectively, with respective capacitances (C). These resistances and capacitances parameters (i.e. R_g, R_{gb}, C_g and C_{gb}) are satisfied the impedance tool from the best fit of the Cole-Cole plots at various temperatures.

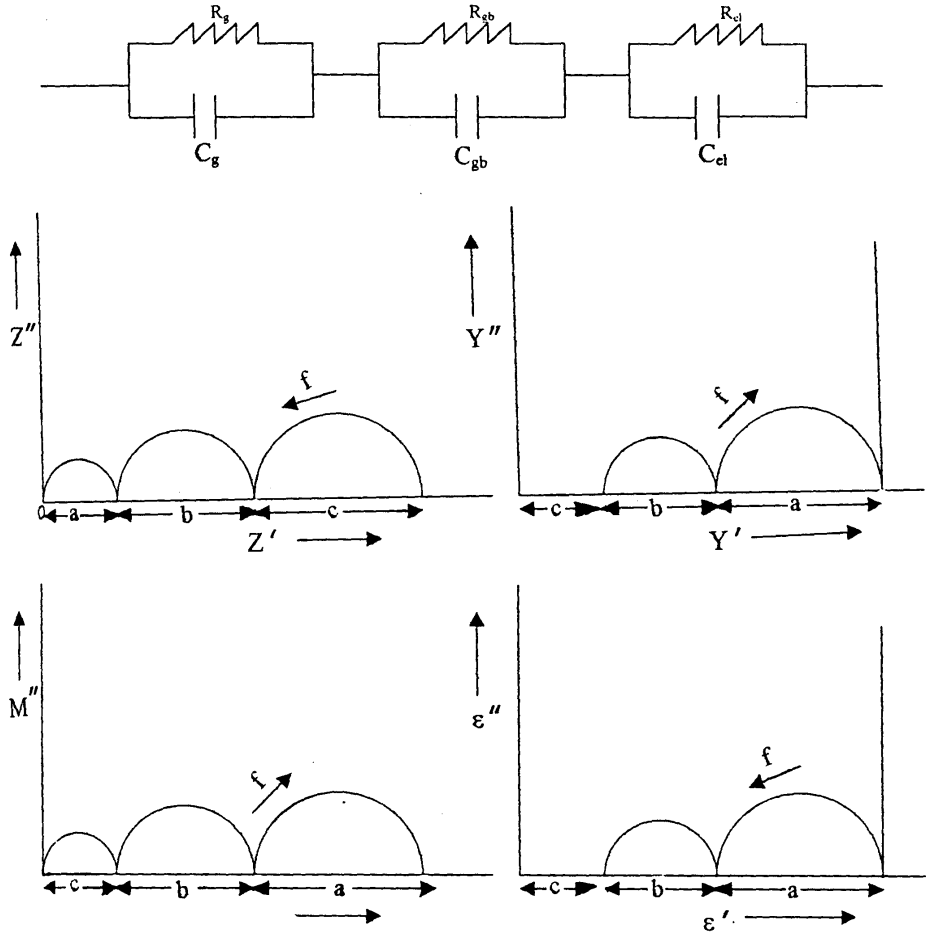

Fig. 2.16: *Equivalent circuit for a polycrystalline ceramic sample and corresponding plots of frequency response in the complex plane [Ref: R. Gerhardt, (1994)].*